High chytrid prevalence and infection intensities in tadpoles of *Mixophyes fleayi*

Matthijs Hollanders, Laura F. Grogan, Hamish I. McCallum, David A. Newell

I Short summary

The amphibian chytrid fungus has descimated frog populations but infection outcome depends on the frog's life stage. We investigated chytrid infection patterns in tadpoles and found that they are often infected with higher pathogen loads than adults and juveniles. This suggests that tadpoles could act as a reservoir for infection and further opens the door to additional research into immune responses of different amphibian life stages. Photo by Matthijs Hollanders.

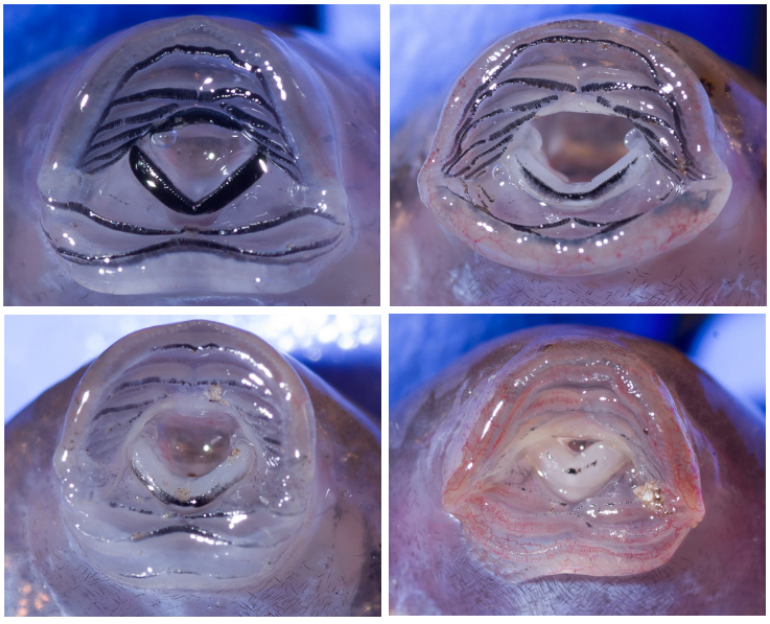

II Abstract

Context: The amphibian chytrid fungus *Batrachochytrium dendrobatidis* (*Bd*) has caused catastrophic biodiversity loss globally, but species and life-stages within species respond differently to the pathogen. Although tadpoles are often reported to be less vulnerable to disease, they can constitute important infection reservoirs in ecosystems.

Aims: We aimed to describe *Bd* infection patterns of a long-lived tadpole in a species where post-metamorphic animals appear to exhibit limited mortality due to chytridiomycosis. We further investigated how oral dekeratinisation can be used as an indicator for infection.

Methods: We conducted surveys over two years for tadpoles of *Mixophyes fleayi* (Fleay's barred frog) at two rainforest streams on the east coast of Australia to assess patterns in *Bd* infection prevalence and intensity. We developed an integrated hierarchical model propagating pathogen detection errors and incorporated how *Bd* infections affect oral dekeratinisation.

Key results: We found that *Bd* infection prevalence was strongly associated with lower temperatures and larger body size, consistent with *Bd* optimal thermal range and a cumulative risk of exposure for tadpoles. The individual probability of a tadpole being infected with *Bd* was estimated to be 0.58 [95% HPDI: 0.432, 0.713], approximately 8 times greater than for adults at the same sites. Tadpoles infected with *Bd* were 113 [29, 293] times more likely have oral dekeratinisation than uninfected tadpoles, where uninfected individuals were estimated to have a 0.05 [95% HPDI: 0.011, 0.11] probability of having mouthpart loss.

Conclusions: Our results show that *M. fleayi* tadpoles are more likely to be infected with *Bd* than adults, suggesting that tadpoles could contribute to *Bd* maintenance in streams. We further show that sites can be rapidly assessed for *Bd* by visually checking for oral dekeratinisation.

Implications: Long-lived tadpoles in general may contribute to *Bd* maintenance in ecosystems. We suggest continued exploration of *Bd* immunocompetence across amphibian life stages to further understand the vastly different infection patterns.

Keywords: *Batrachochytrium dendrobatidis*, tadpole, amphibian, chytridiomycosis, dekeratinisation, pathogen load, mouthpart loss, pathogen detection

III Introduction

The global invasion of the pathogenic amphibian chytrid fungus (*Batrachochytrium dendrobatidis*, *Bd*) has strongly impacted frog species around the world (Berger *et al.* 1998; Scheele *et al.* 2019). However, where some species have been decimated or even driven extinct, others appear to incur fewer costs due to the fungus. Moreover, different life stages present heterogeneity in vulnerability to mortality: where post-metamorphic stages are frequently cited as being more vulnerable—particularly around metamorphosis itself—larval stages (hereafter interchangeably used with tadpoles) experience fewer detrimental effects (Garner *et al.* 2009; Ortiz-Santaliestra *et al.* 2013; Sauer *et al.* 2020).

Although *Bd* infections only rarely directly lead to mortality in tadpoles (Blaustein *et al.* 2005; Arellano *et al.* 2017), infections likely still impact them negatively by limiting feeding ability (Cashins 2009; Venesky *et al.* 2009; Hagman and Alford 2015; Harjoe *et al.* 2022), possibly reducing growth and size at metamorphosis (Garner *et al.* 2009), which may impact individuals post-metamorphosis (Altwegg and Reyer 2003 ; Garner *et al.* 2009; Kilpatrick *et al.* 2010; Sauer *et al.* 2020). Given the immune system reorganisation that takes place at metamorphosis (Rollins-Smith 1998), highly infected tadpoles may experience considerable costs around this stage and larval *Bd* infections may further reduce fitness of recently metamorphosed individuals (Garner *et al.* 2009; Briggs *et al.* 2010; Fernández-Loras *et al.* 2017; Sauer *et al.* 2020). Because the fungus only infects keratinised body parts, which in tadpoles only occur in mouthparts, dekeratinisation of oral structures (hereafter interchangeably used with mouthpart loss) caused by *Bd* may be the mechanism that negatively impacts larval feeding ability (Marantelli *et al.* 2004; Cashins 2009; Venesky *et al.* 2009; Harjoe *et al.* 2022). For example, torrent-adapted tadpoles in tropical streams were reported to have decreased body condition with increased oral dekeratinisation, with body condition improving upon the regrowth of oral structures (Cashins 2009). Upon metamorphosis, the distribution of keratin shifts from the mouthparts to the skin, which rapidly becomes infected with *Bd* upon development (Marantelli *et al.* 2004; McMahon and Rohr 2015). Dekeratinisation of the oral structures, in particular when it is observed in the jaw sheaths, has frequently been noted as an indicator for *Bd* infection in tadpoles (Fellers *et al.* 2001; Rachowicz 2002; Marantelli *et al.* 2004; Blaustein *et al.* 2005; Knapp and Morgan 2006; Drake *et al.* 2007; Cashins 2009). However, the extent to which dekeratinisation is a good indicator appears to be species-specific (Navarro-Lozano *et al.* 2018).

In addition to the costs accrued during the larval phase, tadpoles may act as a reservoir for *Bd* in ecosystems when they occur in permanent water bodies, particularly when tadpoles are long-lived (Rachowicz and Vredenburg 2004; Briggs *et al.* 2010; Catenazzi *et al.* 2013; Valencia-Aguilar *et al.* 2016; Courtois *et al.* 2017; Sapsford *et al.* 2018; das Neves-da-Silva *et al.* 2021). Reservoirs—hosts that permanently maintain the pathogen and transmit it to other hosts (Haydon *et al.* 2002)—can greatly influence disease impact by increasing the exposure to susceptible individuals (Gog *et al.* 2002; De Castro and Bolker 2004). When terrestrial habitats seasonally warm up and dry out, becoming unfavourable for *Bd* growth (Piotrowski *et al.* 2004), the prevalence and intensity (measured as pathogen load) of *Bd* infections frequently decreases in adult frogs (Kriger and Hero 2007). However, aquatic environments may maintain lower temperatures and the requisite moisture requirements for *Bd* growth, facilitating the maintenance of *Bd* in ecosystems (Sapsford *et al.* 2018). Tadpoles may therefore remain infected with (and exposed to) *Bd* under conditions that are favourable to the fungus for long periods of time, and have higher infection prevalence than post-metamorphic individuals.

Previous research has found associations between *Bd* infections, tadpole body size, and temperature (Cashins 2009; Catenazzi *et al.* 2013; Valencia-Aguilar *et al.* 2016; Sapsford *et al.* 2018). Larger tadpoles are reportedly more likely to be infected with *Bd*, likely due to the cumulative exposure older tadpoles have accrued to *Bd* zoospores in the water over time (Valencia-Aguilar *et al.* 2016; Sapsford *et al.* 2018). Infections with *Bd* tend to be more common, and infection intensities higher, with lower water temperatures, likely due to the thermal preferences of *Bd* (Sapsford *et al.* 2018). Although both temperature and body size appear to be influential variables, ambiguity remains about the relative contributions of each on both infection prevalence and intensity in tadpoles (Sapsford *et al.* 2018; das Neves-da-Silva *et al.* 2021).

In this study, we assessed the seasonal *Bd* infection prevalence and infection intensity (pathogen load) of tadpoles over two years in two independent streams. We focused on tadpoles of *Mixophyes fleayi* (Fleay's barred frog), an endangered rainforest species for which the *Bd* prevalence, intensity, and impacts on mortality have been intensively assessed in both adult and recently metamorphosed populations (Hollanders *et al.* 2023b; Hollanders *et al.* 2023a). We built a modified version of a recently developed Bayesian hierarchical model to estimate the effect of temperature, body size, and their interaction on *Bd* infections. We also assessed to what extent mouthpart loss can be predicted by *Bd* infection and the uncertainty associated with using

mouthpart loss as a proxy for *Bd* infection. Our results provide valuable insight into *Bd* dynamics of a long-lived tadpole in subtropical stream environments.

IV Methods

Field surveys

We conducted tadpole surveys at six-weekly intervals from September 2019–January 2021 at Brindle Creek, Border Ranges National Park and Tuntable Creek, Nightcap National Park, New South Wales, Australia. At Brindle Creek, we sampled from two adjacent pools separated by a riffle section where adult frogs were known to breed. At Tuntable Creek, we sampled from four pools separated by riffle sections. We used a dipnet (Jonah's Aquarium The Perfect Dipnet, 1/8" mesh) to sample each pool for 1 min.

Tadpoles were held in a plastic tub and up to 40 individuals were processed (photographed and sampled for *Bd*) per site per occasion. For one year at Brindle Creek we took a top-down photograph of the full tub of tadpoles (prior to subsampling 40 for processing) in order to measure the length of each tadpole (from the tip of the nose to the base of the tail) using the Ruler Tool in Adobe Photoshop to gauge the distribution of size classes (Figure 1). We handled tadpoles following Cashins (2009), photographed their mouthparts (Nikon D750 and Sigma 105mm macro at minimum focus), and sampled for *Bd* using swabs (five horizontal strokes and five vertical strokes across the mouthparts). For 620 individuals sampled over the two years, we photographed mouthparts to identify mouthpart loss associated with *Bd* and to derive a body size proxy, for which we used the distance between the two mouth corners measured in pixels using the Ruler Tool in Adobe Photoshop 2020. We chose to measure body size indirectly using this method to reduce handling time of the animals and to get a more precise measurement compared to measuring body length in-hand using calipers. We verified the method by comparing body length measurements using calipers with mouthpart widths measured using Photoshop of 136 individuals and found strong agreement between the two measurements (Figure S1). We identified mouthpart loss by assessing for dekeratinisation of the jaw sheaths from photographs, and scored the amount of dekeratinisation of both the bottom and top jaw sheath on a scale of 1–5 (Figure 2).

We placed dataloggers (HOBO MX2201) along the edge of the stream to record temperature every 2 hrs for the duration of the study. We relied on terrestrial dataloggers for our analysis because dataloggers in the creeks were swept away by floods.

< Figure 2 could go here.>

Laboratory work

We extracted and amplified *Bd* DNA using standard protocols (Boyle *et al.* 2004; Hyatt *et al.* 2007; Brannelly *et al.* 2020). Briefly, DNA was extracted using Prepman® Ultra (Applied Biosystems) without bead-beating step (Brannelly *et al.* 2020). Then, sample DNA was amplified using quantitative Polymerase Chain Reaction (qPCR) in duplicate with synthetic gBlocks ITS reference standards (Integrated DNA Technologies) to quantify *Bd* DNA present on swabs. We considered samples positive when at least one qPCR well returned *Bd* DNA. Infection intensities are reported as $\log_{10}$ gene copies per swab. For further details on the laboratory process, see Hollanders *et al.* (2023b).

Statistical analysis

To identify patterns in *Bd* infection status (infected/uninfected) and infection intensity (pathogen load), we fit a model to swab infection status and ($\log_{10}$) swab infection intensities, respectively, correcting for measurement error in the qPCR and the sampling processes (DiRenzo *et al.* 2018, Appendix S2). The model incorporated imperfect pathogen detection in the qPCR process through both false-negatives and false-positives, and further introduced measurement error in the swab infection intensities using an informative prior, because infection intensities measured from single samples may not accurately reflect the true infection intensities of individuals (DiRenzo *et al.* 2018; McElreath 2020; Hollanders 2022). Note that although infection status was corrected for imperfect detection due to qPCR, we did not model the false-negatives associated with the swabbing protocol; however, double-swabbing tadpoles would likely not have yielded independent samples (Hollanders 2022).

The model featured a logistic regression component to latent infection status and a linear regression to latent individual infection intensities (see Appendix S2 for details). Both regression models included site, average temperature over the six-week survey intervals, (log) tadpole size (using the proxy of mouthpart width), all pairwise interactions, the three-way interaction, and correlated random survey effects as predictors. We modeled both the presence (binary) and intensity (ordinal) of mouthpart loss, as determined by the presence and degree of dekeratinization of the jaw sheath (summed over both top and bottom), as descendant variables of *Bd* infection. Each component was modeled as a function (logit-linear for status and ordered

probit for intensity) of latent estimated *Bd* infection intensity (and infection status for presence only) and correlated random survey effects. Additionally, we included effects of body size separately for infected and uninfected tadpoles. We conducted posterior predictive checks for the four components of the model and calculated Bayesian *p*-values for each to assess goodness-of-fit (Gelman *et al.* 1996, Appendix S2).

We implemented the model with Bayesian methods using NIMBLE 1.0.1 (de Valpine *et al.* 2017; de Valpine *et al.* 2023) through R 4.3.0 (R Core Team 2023) with weakly informative priors (except for the measurement error of the swabbing process, Table 1, Appendix S2). For predictor variable selection, we used NIMBLE's built-in reversible jump MCMC (RJMCMC, Green 1995) samplers, which excludes parameters that do not contribute sufficiently to the likelihood (and toggles values to 0 for those iterations where parameters are excluded). Predictors were centered and scaled by two standard deviations to allow direct comparison between binary (site) and continuous (temperature and body size) effects (Gelman *et al.* 2008). We imputed missing body size values ($n = 244$) from a normal distribution parameterized from observed values ($n = 621$) using MCMC. We ran 4 chains for 50,000 iterations after discarding 10,000 as burn-in and thinning chains by 10, yielding 20,000 posterior samples which resulted in convergence of all model parameters. We summarized posterior distributions with medians and 95% highest posterior density intervals (HPDIs), included the samples where RJMCMC toggled coefficients to 0 in these summary statistics, report the RJMCMC inclusion probabilities, and considered effects important when 95% HPDIs of the coefficients did not overlap 0. The analysis is fully reproducible on https://github.com/mhollanders/mfleayi-tadpoles.

< Figure 1 could go here.>

V Results

Sampling summary

We captured and swabbed 865 *M. fleayi* tadpoles (424 at Brindle and 441 at Tuntable) over 25 surveys. Of those, 54% (471) returned *Bd* DNA in at least one qPCR run, with the median *Bd* infection intensity being 4.02 $\log_{10}$ gene copies per swab (averaged over duplicate qPCR runs). Of the 620 tadpoles sampled for mouthpart loss, 39% (243) showed dekeratinisation: of those, 95% (230) returned *Bd* in at least one qPCR replicate. Because tadpoles were not marked, some individuals may have been sampled more than once over the study period. Tadpoles were present year-round, with pulses of reproduction occurring in Austral spring and autumn (Figure 1).

Bd infection prevalence

Average *Bd* prevalence was estimated as 0.58 [95% HPDI: 0.432, 0.713], with no significant site effect (log odds change 0 [95% HPDI: -1.009, 0.828], RJMCMC inclusion 0.551) (Table 1). Individual probability of being infected with *Bd* was strongly negatively associated with temperature (log odds change -3.271 [95% HPDI: -4.616, -1.943], RJMCMC inclusion 1) and strongly positively with body size (log odds change 3.966 [95% HPDI: 3.129, 4.891], RJMCMC inclusion 1) (Table 1, Figure 4). We found weak evidence for interaction effects, with low RJMCMC inclusion probabilities and effect estimates overlapping 0 (Table 1). The Bayesian *p*-value of the prevalence component of the model was 0.293, indicating reasonable fit (Appendix S2, Figure S3a). Model fit improved significantly with the addition of the random survey effect (comparison not shown), which was large (standard deviation [SD] of the effect 1.257 [95% HPDI: 0.788, 1.853]), suggesting a considerable amount of unexplained variation between surveys (Figure 3a). The survey effects were somewhat positively correlated with those of infection intensity (correlation of 0.235 [95% HPDI: -0.307, 0.727]), suggesting that when infection were common the associated infection intensities were also relatively high. The probability of detecting *Bd* using qPCR was high (probability of detecting one $\log_{10}$ gene copy in a qPCR replicate estimated as 0.619 [95% HPDI: 0.567, 0.677], yielding a 0.999 [95% HPDI: 0.999, 1] probability of

detecting the average load after two qPCR replicates), reflected in that the model estimated that 460 individuals were infected compared to the 471 infections that we observed. The false-positive probability of detecting *Bd* in the qPCR protocol was estimated low (0.016 [95% HPDI: 0.003, 0.029]), but note that *Bd* detection errors in the swabbing process was not modeled because only single swabs were collected.

< Figure 4 could go here.>

Bd infection intensity

Average *Bd* infection intensity was estimated as 3.88 [95% HPDI: 3.68, 4.07] $\log_{10}$ gene copies, with no significant differences between sites (RJMCMC inclusion 0.33), with a population SD of 1.56 [95% HPDI: 1.44, 1.69] (Table 1). There was a weak positive association between individual *Bd* infection intensity and body size (log change 0.45 [0.22, 0.69], RJMCMC inclusion 1) (Figure S2) but no association with temperature (log change 0 [95% HPDI: -0.44, 0.12], RJMCMC inclusion 0.29). We found no evidence for interaction effects, and unexplained variation in the form of survey effects was small (SD of survey effect 0.42 [95% HPDI: 0.28, 0.57]) (Table 1, Figure 3b). There was some measurement error associated with the qPCR process (SD of effect 0.63 [95% HPDI: 0.59, 0.67]), and together with the additional swabbing measurement error (0.12 [95% HPDI: 0, 0.24]) incorporated into the model with an informative prior, there were considerable differences between the observed swab infection intensities (computed as the sample mean of positive qPCR replicates) and the estimated latent individual infection intensities (Figure S2). The Bayesian p-value for this model was 0.76, suggesting decent fit (Appendix S2, Figure S3b).

Mouthpart loss

The presence of mouthpart loss, specifically determined by dekeratinisation of the jaw sheath, was strongly influenced by *Bd* infection. Uninfected individuals had a probability of 0.05 [95% HPDI: 0.01, 0.11] of having mouthpart loss, where infected tadpoles (carrying the average *Bd* infection intensity) had a 0.85 [95% HPDI: 0.7, 0.97] probability (log odds change 4.73 [95% HPDI: 3.66, 5.77], RJMCMC inclusion 1) (Table 1, Figure 5a). This implies that individuals infected with *Bd* had 113 [95% HPDI: 29, 293] times greater odds to have dekeratinisation of the jaw sheath than

uninfected individuals, and that there was a 0.15 [95% HPDI: 0.03, 0.3] probability of tadpoles infected with *Bd* to not have dekeratinisation. For those individuals that were infected with *Bd*, higher *Bd* infection intensities were associated with a considerably higher probability of mouthpart loss (log odds change 2.54 [95% HPDI: 1.31, 3.97], RJMCMC inclusion 1) (Figure 5b). Body size was not found to have a direct effect on the probability of mouthpart loss. There was a large amount of unexplained survey variation (SD of survey effect 1.83 [1.09, 2.76]), which was strongly correlated with those of mouthpart loss intensity (0.7 [95% HPDI: 0.34, 0.95]), showing that when many tadpoles had some degree of mouthpart loss that the intensity of mouthpart loss was high (Figure 3c–d). The Bayesian *p*-value of this component was 0.62, suggesting good fit (Appendix S2, Figure S3c).

Finally, the intensity of mouthpart loss, as determined by the amount of dekeratinisation in the jaw sheaths, was associated with *Bd* infection status but infection status could not be included as a predictor due to the lack of uninfected individuals with mouthpart loss (Figure 5c). Infection intensity was weakly positive associated with degree of oral dekeratinisation (standardised change 0 [-0.02, 0.71], RJMCMC inclusion 0.41). For uninfected tadpoles, body size was positively associated with the degree of oral dekeratinisation (standardised change 0.91 [0, 1.93], RJMCMC inclusion 0.81). There was some amount of unexplained survey variation (SD of survey effect (1.22 [0.8, 1.74]). Goodness-of-fit of this component was good (Bayesian *p*-value 0.31) (Appendix S2, Figure S3d).

< Figure 5 could go here.>

VI Discussion

We investigated the occurrence of *Bd* and associated infected intensities in endangered *Mixophyes fleayi* tadpoles over two years, and found that both average infection prevalence (0.58 [95% HPDI: 0.43, 0.71]) and infection intensity (3.88 [3.68, 4.07] $\log_{10}$ gene copies per swab) were high. Compared to adults from the same sites reported in previous studies—which had an average reported prevalence of 0.15 [95% HPDI: 0.07, 0.27] and intensity of 3.036 [95% HPDI: 2.836, 3.234] (Hollanders *et al.* 2023b)—the odds of tadpoles being infected with *Bd* were approximately 8 times greater and average $\log_{10}$ infection intensities were 1.28 times greater. We found evidence of seasonality for *Bd* infections in tadpoles, where lower temperatures were associated with higher *Bd* prevalence (but not *Bd* infection intensity). Additionally, we corroborated evidence for risk of infection increasing cumulatively with age, as we found a strong association between body size and infection prevalence. It is noteworthy that recently metamorphosed *M. fleayi* at Brindle Creek have lower average infection prevalence (estimated at 0.42 [95% HPDI: 0.13, 0.7] after correcting for imperfect detection in the swabbing process) and lower infection intensities (estimated at 2.8 [2.45, 3.08] $\log_{10}$ gene copies per swab) than the tadpoles (Hollanders *et al.* 2023a). This discrepancy of infection patterns between larval and post-metamorphic individuals sharing a spatio-temporal space warrants further investigation and suggests considerable differences in immunocompetence, pathogen resistance, exposure history, or other mechanisms of persistence (Brannelly *et al.* 2021).

Individual *Bd* infections of tadpoles was associated with lower temperatures and larger body sizes, consistent with results from previous studies (Figure 4) (Cashins 2009; Catenazzi *et al.* 2013; Valencia-Aguilar *et al.* 2016; Sapsford *et al.* 2018). Low temperatures also correlated with increased infection prevalence with adult amphibians at the same site, consistent with the regional pattern previously reported (Kriger and Hero 2007; Hollanders *et al.* 2023b). The average six-weekly temperatures at the sites ranged from 8.6–19.8°C, which is within the optimal range for *Bd* growth; nevertheless, growth is reportedly faster around 20°C than it is around 10°C, so *Bd* physiology may explain the observed pattern of infection prevalence at our sites (Piotrowski *et al.* 2004; Stevenson *et al.* 2013). However, thermal optima vary among *Bd* strains and the performance of the local strain is unknown (Voyles *et al.* 2017). Alternatively, immune function of tadpoles may be improved with higher temperatures (Cohen *et al.* 2017). Although tadpole immune response to *Bd* is poorly understood, previous studies demonstrated that

low-protein diets increased the probability of gaining *Bd* infections (Venesky *et al.* 2012) and tadpoles kept at lower temperatures had higher infection intensities (Altman and Raffel 2019), suggesting resistance to *Bd* is influenced by external factors. Further, some studies have reported regrowth of oral structures after initial dekeratinisation due to *Bd* infection, suggesting possible immune response after infection (Cashins 2009; Hagman and Alford 2015). However, if tadpoles mounted successful immune responses to *Bd* infection, lower probability of being infected would be expected with larger body size, and/or lower infection intensities would be associated with these remaining infections. Contrary to this, we found evidence for infection status being strongly predicted by body size (a proxy for age), in line with previous studies (Valencia-Aguilar *et al.* 2016; Sapsford *et al.* 2018). This result is consistent with tadpoles experiencing a cumulative exposure risk and limited immune response to suppress *Bd* infections in the field.

Unlike infection status, we did not find strong predictors influencing infection intensity. RJMCMC excluded all predictors except body size, which was found to have a weakly positive effect on infection intensity (Figure S2); however, this may simply reflect that larger tadpoles have larger oral structures to swab. The lack of evidence for a temperature effect was noteworthy given the strength of the effect of temperature on infection status. This may reflect that *Bd* growth is largely independent of the range of temperatures that occur in these streams once *Bd* becomes established on a tadpole. Tadpoles did have considerably higher average infection intensities than adults (median of 3.88 vs. 3.0 $\log_{10}$ gene copies), which may in fact underestimate the difference given that tadpoles only have their oral structures swabbed (10 strokes) compared with the entire ventral surface of post-metamorphic animals (45 strokes, Hollanders *et al.* 2023b). That tadpoles in populations where adults display limited susceptibility to *Bd* after initial epidemics have higher infection intensities than adult frogs has also been found in *Rana sierrae/muscosa* in the United States (Briggs *et al.* 2010). One explanation is that tadpoles exist in an environment that is more conducive to *Bd* growth due to the moisture and lower temperatures (Piotrowski *et al.* 2004). Alternatively, an increased immune response may be present in adult individuals compared to tadpoles. With relatively fewer deleterious consequences of *Bd* infections for tadpoles, lower selective pressure would be expected compared to post-metamorphic animals experiencing mortality due to chytridiomycosis. Our results indicate that subtropical stream environments are suitable for high *Bd* prevalence in tadpoles throughout the year.

Tadpoles of *Mixophyes fleayi* may be an important *Bd* reservoir due to the high infection

prevalence and intensity and year-round presence in the streams (Rachowicz and Vredenburg 2004; Cashins 2009; Briggs *et al.* 2010; Catenazzi *et al.* 2013; Courtois *et al.* 2017; Sapsford *et al.* 2018). However, without an explicit causal or mechanistic model that accounts for transmission (i.e., shedding rates, exposure rates of vulnerable hosts, etc.), we cannot make claims about their status as a reservoir (Wilber *et al.* 2022). Based on the body size distributions from December 2019–January 2021, pulses of reproduction occurred in the summer months (Figure 1), consistent with previous studies (Stratford *et al.* 2010). Importantly, large tadpoles were present throughout the study period; given that larger tadpoles were more often infected, these individuals likely contribute to the maintenance of *Bd* in the stream environments. Experimental studies have shown that tadpoles readily infect other tadpoles when they share an aquatic environment (Rachowicz and Briggs 2007; Hagman and Alford 2015; Courtois *et al.* 2017). However, the extent to which adults become infected when entering these aquatic environments is less well understood. In laboratory studies, all post-metamorphic animals housed in an enclosure with infected tadpoles became infected within three weeks (Rachowicz and Vredenburg 2004). However, the transmission of tadpoles to terrestrial adults is currently poorly understood. For stream-breeding frogs where breeding congregations occur in and around streams, understanding the risk of exposure from the stream environment is important for understanding infection dynamics. This remains an open area of research across many *Bd*-amphibian systems.

To our knowledge, our study is the first to assess the effects of both *Bd* infection status and intensity on the probability of having oral dekeratinisation. Our results confirm that oral dekeratinisation is a good indicator of *Bd* infection in *Mixophyes fleayi*, with a 0.15 [95% HPDI: 0.03, 0.3] probability of an infected tadpole not displaying oral dekeratinisation (Symonds *et al.* 2007; Navarro-Lozano *et al.* 2018). We found that infected tadpoles had on average 113 times higher odds to have mouthpart loss than uninfected tadpoles (Figure 5a). Additionally, we found that among those tadpoles infected with *Bd*, individuals with a higher infection intensity were significantly more likely to have mouthpart loss (Figure 5b). Only 13 tadpoles that had oral dekeratinisation returned negative swabs, but some of these were likely to be false-negatives. Our study did not correct for *Bd* detection errors in the swabbing process, which is predicted to be roughly 0.67 for the average tadpole infection intensity estimated in this study (Hollanders *et al.* 2023a). Although other causes of oral dekeratinisation exist (Knapp and Morgan 2006), given the prevalence of *Bd* at our sites and the clear association with *Bd*, these individuals likely lost their mouthparts due to infection. The positive effect of body size on the degree of oral

dekeratinisation for uninfected tadpoles may also suggest that prior infections caused the dekeratinisation, and that tadpoles had successfully cleared infection or that our detection protocol failed to detect *Bd* in these tadpoles. Importantly, the probability of finding two tadpoles with oral dekeratinisation that are not infected with *Bd* is just 0.0025; consequently, the presence of mouthpart loss in a small sample of tadpoles should allow investigators to conclude the presence of *Bd*. Unfortunately, the relationship between oral dekeratinisation and *Bd* infection appears highly species-specific: although the relationship is present for many species, some species show mouthpart loss in the absence of *Bd* (Navarro-Lozano *et al.* 2018).

In conclusion, we have shown that *Bd* infection prevalence and infection intensity in tadpoles are considerably higher than for adults and juveniles at the same sites. Our focal species *Mixophyes fleayi* declined significantly during the epidemic but has since recovered, having stable populations despite individual mortality occurring with high *Bd* intensities (Hollanders *et al.* 2023b). Nevertheless, the year-round presence of tadpoles that are more often infected and infected with higher pathogen loads in the stream environments may constitute a *Bd* reservoir, both in terms of indirect transmission through the water and directly into the adult population through metamorphosis. However, to establish the role of tadpoles as pathogen reservoirs, future research will need to quantify transmission to more vulnerable hosts. The results of this work suggest fruitful future research into mechanisms of immunocompetence across amphibian life stages

VII Ethics

Field surveys were performed under New South Wales Scientific License 102444 with Southern Cross University Animal Care and Ethics Committee approval (Animal Research Authority 20034).

VIII Data availability statement

All data, analysis scripts, and posterior samples are available at https://github.com/mhollanders/mfleayi-tadpoles.

IX Conflicts of interests

The author have no conflicts of interests to report.

X Declaration of funding

This project was funded by the New South Wales Government's Saving our Species program wish specific thanks to Jill Smith and David Hunter. L.G. was supported by Australian Research Council (ARC) grants DP180101415 and DE200100490. H.M. and D.N. were supported by ARC grant DP180101415.

XI Acknowledgements

We extend special thanks to New South Wales National Parks and Wildlife Service for allowing us to conduct field work. We thank volunteers Darren McHugh, Liam Bolitho, Madelyn Mangan, and Josephine Humphries for asisstance in the field.

XII Tables

Table 1: Posterior (with median and 95% HPDI) and prior distributions for the *Bd* infection status and intensity and the mouthpart loss status and intensity model components. Stars indicate predictors for which the 95% HPDI did not overlap 0. The *Bd* detection probability (r) is the probability of detecting one $\log_{10}$ gene copy of *Bd* in a qPCR run, and the false positive probability (δ_{21}) is the probability of getting a positive detection during qPCR when the sample was not truly infected with *Bd*.

Function	**Parameter**	**Median**	**95% HPDI**	**RJMCMC**	**Prior**
Bd infection status (ψ)					
	Intercept	0.58	[0.432, 0.713]		Beta$(3, 3)$
	Temp*	-3.271	[-4.616, -1.943]	1	$t_3(0, 1)$
	Body size*	3.966	[3.129, 4.891]	1	$t_3(0, 1)$
	Site	0	[-1.009, 0.828]	0.551	$t_3(0, 1)$
	Temp × body size	0	[-1.609, 0.776]	0.443	$t_3(0, 1)$
	Temp × site	0	[-0.658, 1.879]	0.33	$t_3(0, 1)$
	Body size × site	0	[-1.142, 0.633]	0.293	$t_3(0, 1)$
	Temp × body size × site	0	[-1.46, 0.39]	0.125	$t_3(0, 1)$
	Survey (SD)	1.257	[0.788, 1.853]		$t_3^+(0, 1)$
	Bd detection probability (r)	0.619	[0.567, 0.677]		Beta$(6, 4)$
	Bd false-positive (δ_{21})	0.016	[0.003, 0.029]		Beta$(1, 10)$
Bd infection intensity (μ)					
	Intercept	3.88	[3.685, 4.069]		$t_3(4, 1)$
	Temp	0	[-0.444, 0.116]	0.291	$t_3(0, 1)$
	Body size*	0.45	[0.222, 0.692]	0.996	$t_3(0, 1)$
	Site	0	[-0.417, 0.106]	0.326	$t_3(0, 1)$
	Temp × body size	0	[-0.205, 0.117]	0.104	$t_3(0, 1)$
	Temp × site	0	[-0.092, 0.228]	0.083	$t_3(0, 1)$
	Body size × site	0	[-0.38, 0.017]	0.122	$t_3(0, 1)$
	Temp × body size × site	0	[0, 0]	0.049	$t_3(0, 1)$
	Survey (SD)	0.415	[0.281, 0.571]		$t_3^+(0, 1)$
	Population SD ($\exp \sigma_\mu$)	1.564	[1.439, 1.687]		$t_3^+(0, 1)$
	Swab error (σ_{swab})	0.121	[0, 0.242]		$t_3^+(0.17, 0.11)$
	qPCR error (σ_{qPCR})	0.632	[0.593, 0.672]		$t_3^+(0.5, 0.05)$

Function	**Parameter**	**Median**	**95% HPDI**	**RJMCMC**	**Prior**
Mouthpart loss status (λ)					
	Intercept	0.05	[0.011, 0.11]		Beta$(1, 10)$
	Bd infection status*	4.727	[3.656, 5.772]	1	$t_3(0, 1)$
	Bd infection intensity*	2.541	[1.31, 3.969]	1	$t_3(0, 1)$
	Body size (if *Bd*+)	0	[-0.809, 0.869]	0.333	$t_3(0, 1)$
	Body size (if *Bd*–)	0	[-0.75, 0.934]	0.35	$t_3(0, 1)$
	Survey (SD)	1.826	[1.088, 2.762]		$t_3^+(0, 1)$
Mouthpart loss intensity (κ)					
	Bd infection intensity	0	[-0.023, 0.715]	0.412	$t_3(0, 1)$
	Body size (if *Bd*+)	0	[-0.329, 0.359]	0.218	$t_3(0, 1)$
	Body size (if *Bd*–)*	0.912	[0, 1.928]	0.807	$t_3(0, 1)$
	Survey (SD)	1.218	[0.803, 1.742]		$t_3^+(0, 1)$

XIII Figures

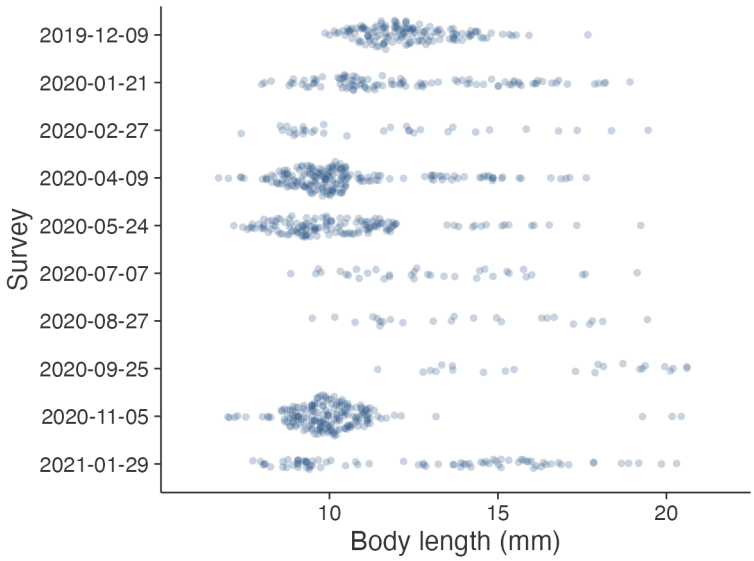

Figure 1: Size distributions of *Mixophyes fleayi* tadpoles per survey at Brindle Creek over one year.

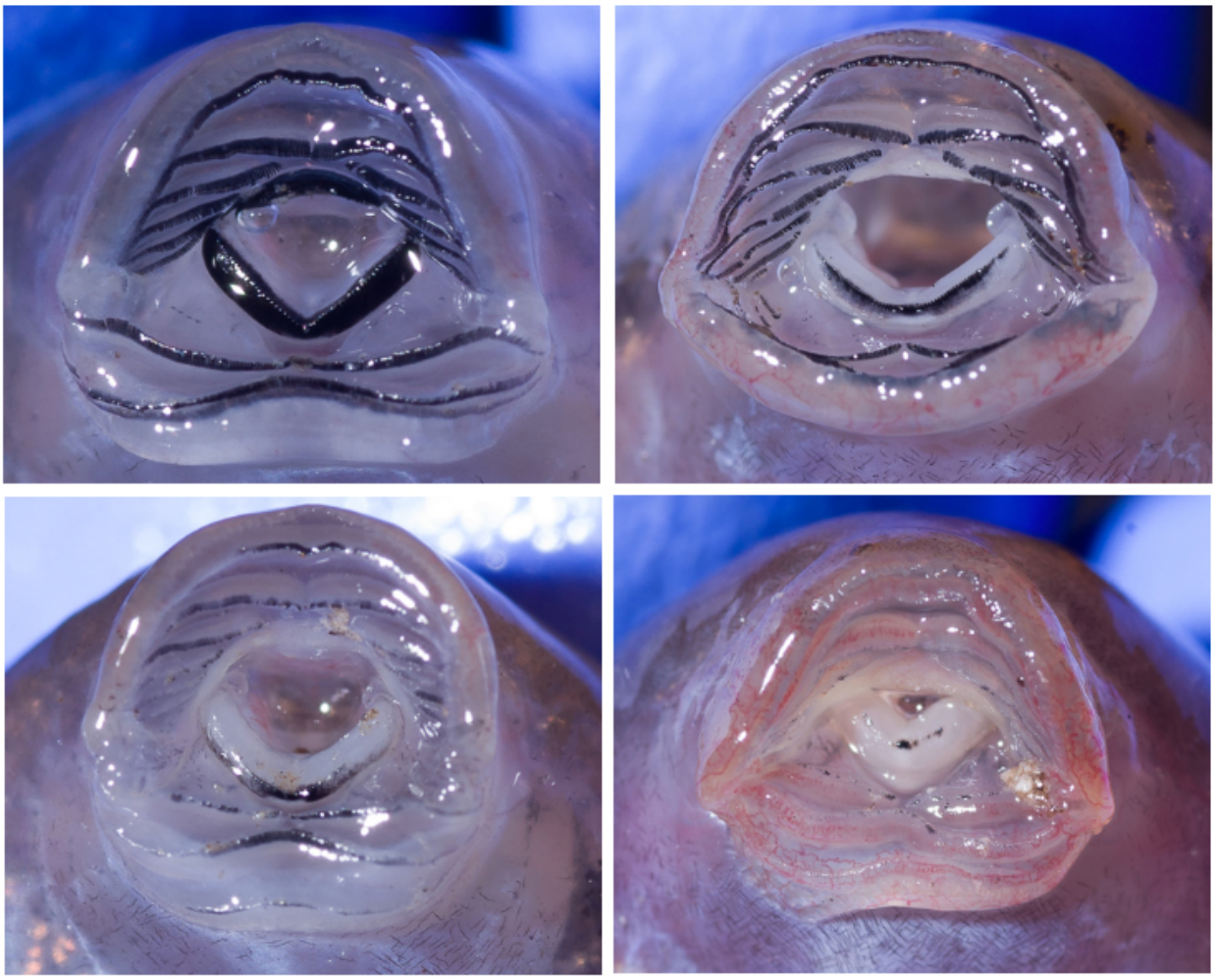

Figure 2: Various stages of oral dekeratinization in tadpoles of *Mixophyes fleayi*. The oral dekeratinisation scores of top/bottom jaw sheats were **(a)** NA/NA, **(b)** 1/3, **(c)** 3/4, and **(d)** 5/5.

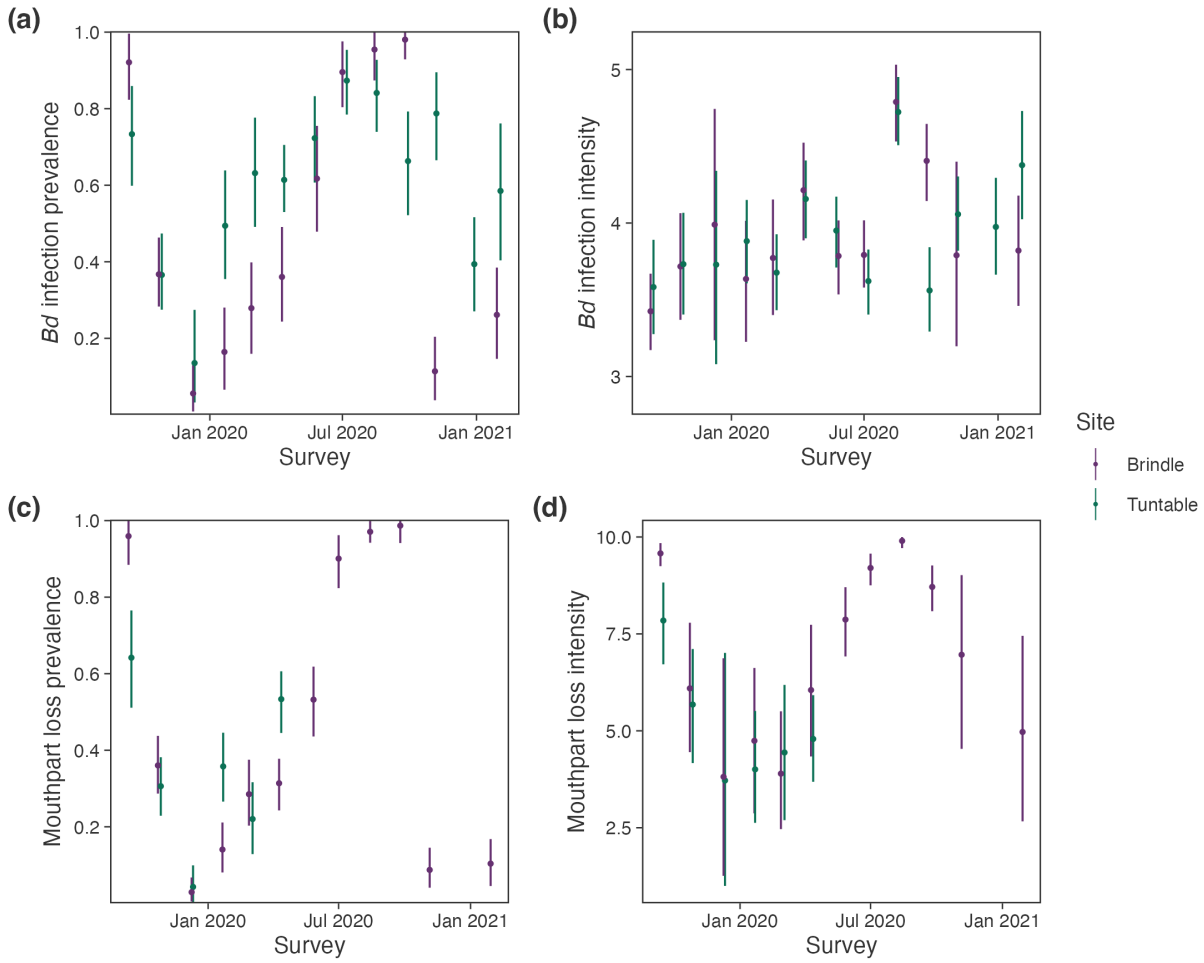

Figure 3: Survey-specific estimates (medians and 95% HPDIs) of **(a)** *Bd* infection prevalence, **(b)** average *Bd* infection intensity ($\log_{10}$ gene copies per swab), **(c)** oral dekeratinisation prevalence, and **(d)** average oral dekeratinisation score of tadpoles with dekeratinisation. Estimates were averaged over individual-level predictions for each survey.

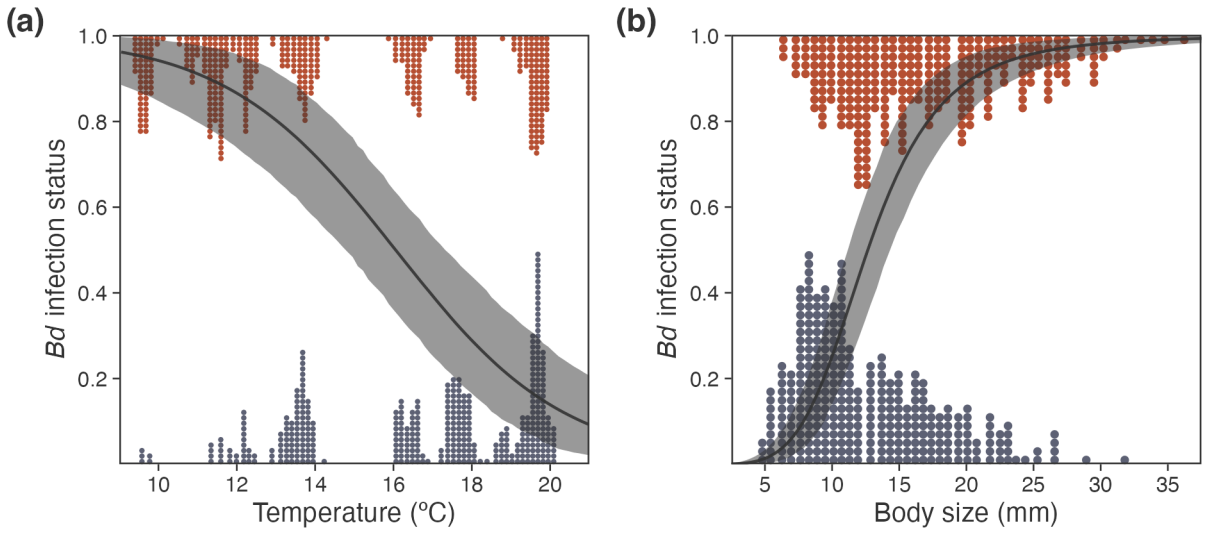

Figure 4: Prediction curves (medians and 95% HPDIs) with the coefficients of temperature **(a)** and body size **(b)** on the probability of *Mixophyes fleayi* tadpoles being infected with *Bd* from logistic regression, with the other (scaled) predictors held at their respective means. Points are observed individuals with corresponding temperature **(a)** and body size **(b)** at observation, categorised by *Bd* infection status (infected, top; uninfected, bottom). Body sizes were transformed from mouthpart widths using the equation in Figure S1.

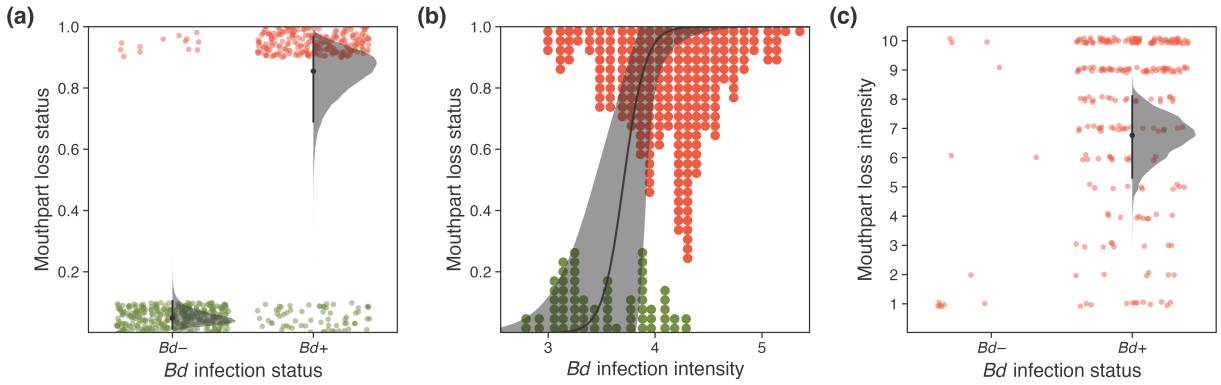

Figure 5: **(a)** Posterior distributions (with medians and 95% HPDIs) of the probability of having mouthpart loss, as determined by the presence of dekeratinisation of the jaw sheath, for *Mixophyes fleayi* tadpoles uninfected (left) and infected (right) with *Bd*. Jittered points are observed individuals, categorised by presence of mouthpart loss (present, top; absent, bottom) and *Bd* infection status. **(b)** Prediction curve (median and 95% HPDI) with the coefficient of *Bd* infection intensity on the probability of having mouthpart loss from logistic regression. Points are observed individuals with corresponding *Bd* infection intensities estimated by the model (summarised as the median of the posterior distributions) after accounting for measurement error in the sampling (swabbing) and diagnostic (qPCR) processes. **(c)** Posterior distribution (with median and 95% HPDI) of the average mouthpart loss intensity score for infected (right) tadpoles (there was not enough data to estimate the score of uninfected tadpoles). Points are observed mouthpart loss intensity scores.

XIV References

Altman KA, Raffel TR (2019). Thermal acclimation has little effect on tadpole resistance to *Batrachochytrium dendrobatidis*. *Diseases of Aquatic Organisms* **133**, 207–216. doi:10.3354/dao03347

Altwegg R, Reyer H-U (2003). Patterns of natural selection on size at metamorphosis in water frogs. *Evolution* **57**, 872–882. doi:10.1111/j.0014-3820.2003.tb00298.x

Arellano ML, Natale GS, Grilli PG, Barrasso DA, Steciow MM, Lavilla EO (2017). Host-pathogen relationships between the chytrid fungus *Batrachochytrium dendrobatidis* and tadpoles of five South American anuran species. *Herpetological Journal* **27**, 33–39.

Berger L, Speare R, Daszak P, Green DE, Cunningham AA, Goggin CL, Slocombe R, Ragan MA, Hyatt AD, McDonald KR, Hines HB, Lips KR, Marantelli G, Parkes H (1998). Chytridiomycosis causes amphibian mortality associated with population declines in the rain forests of Australia and Central America. *Proceedings of the National Academy of Sciences* **95**, 9031–9036. doi:10.1073/pnas.95.15.9031

Blaustein AR, Romansic JM, Scheessele EA, Han BA, Pessier AP, Longcore JE (2005). Interspecific variation in susceptibility of frog tadpoles to the pathogenic fungus *Batrachochytrium dendrobatidis*. *Conservation Biology* **19**, 1460–1468. doi:10.1111/j.1523-1739.2005.00195.x

Boyle DG, Boyle DB, Olsen V, Morgan JAT, Hyatt AD (2004). Rapid quantitative detection of chytridiomycosis (*Batrachochytrium dendrobatidis*) in amphibian samples using real-time Taqman PCR assay. *Diseases of Aquatic Organisms* **60**, 141–148. doi:10.3354/dao060141

Brannelly LA, McCallum HI, Grogan LF, Briggs CJ, Puig Ribas M, Hollanders M, Sasso T, Familiar López M, Newell DA, Kilpatrick AM (2021). Mechanisms underlying host persistence following amphibian disease emergence determine appropriate management strategies. *Ecology Letters* **24**, 130–148. doi:10.1111/ele.13621

Brannelly LA, Wetzel DP, West M, Richards-Zawacki CL (2020). Optimized *Batrachochytrium dendrobatidis* DNA extraction of swab samples results in imperfect detection particularly when infection intensities are low. *Diseases of Aquatic Organisms* **139**, 233–243. doi:10.3354/dao03482

Briggs CJ, Knapp RA, Vredenburg VT (2010). Enzootic and epizootic dynamics of the chytrid fungal pathogen of amphibians. *Proceedings of the National Academy of Sciences* **107**,

9695–9700. doi:10.1073/pnas.0912886107

Cashins SD (2009). Epidemiology of Chytridiomycosis in rainforest stream tadpoles. PhD thesis, James Cook University.

Catenazzi A, von May R, Vredenburg VT (2013). High prevalence of infection in tadpoles increases vulnerability to fungal pathogen in high-Andean amphibians. *Biological Conservation* **159**, 413–421. doi:10.1016/j.biocon.2012.11.023

Cohen JM, Venesky MD, Sauer EL, Civitello DJ, McMahon TA, Roznik EA, Rohr JR (2017). The thermal mismatch hypothesis explains host susceptibility to an emerging infectious disease. *Ecology Letters* **20**, 184–193. doi:10.1111/ele.12720

Courtois EA, Loyau A, Bourgoin M, Schmeller DS (2017). Initiation of *Batrachochytrium dendrobatidis* infection in the absence of physical contact with infected hosts – A field study in a high altitude lake. *Oikos* **126**, 843–851. doi:10.1111/oik.03462

das Neves-da-Silva D, Borges-Júnior VNT, Branco CWC, de Carvalho-e-Silva AMPT (2021). Effects of intrinsic and extrinsic factors on the prevalence of the fungus *Batrachochytrium dendrobatidis* (Chytridiomycota) in stream tadpoles in the Atlantic Forest domain. *Aquatic Ecology* **55**, 891–902. doi:10.1007/s10452-021-09869-y

De Castro F, Bolker B (2004). Mechanisms of disease-induced extinction. *Ecology Letters* **8**, 117–126. doi:10.1111/j.1461-0248.2004.00693.x

de Valpine P, Paciorek C, Turek D, Michaud N, Anderson-Bergman C, Obermeyer F, Wehrhahn Cortes C, Rodrìguez A, Temple Lang D, Paganin S (2023). NIMBLE: MCMC, particle filtering, and programmable hierarchical modeling. manual. doi:10.5281/zenodo.1211190

de Valpine P, Turek D, Paciorek CJ, Anderson-Bergman C, Lang DT, Bodik R (2017). Programming with models: Writing statistical algorithms for general model structures with NIMBLE. *Journal of Computational and Graphical Statistics* **26**, 403–413. doi:10.1080/10618600.2016.1172487

DiRenzo GV, Campbell Grant EH, Longo AV, Che-Castaldo C, Zamudio KR, Lips KR (2018). Imperfect pathogen detection from non-invasive skin swabs biases disease inference. *Methods in Ecology and Evolution* **9**, 380–389. doi:10.1111/2041-210X.12868

Drake DL, Altig R, Grace JB, Walls SC (2007). Occurrence of oral deformities in larval anurans. *Copeia* **2007**, 449–458. doi:10.1643/0045-8511(2007)7[449:OOODIL]2.0.CO;2

Fellers GM, Green DE, Longcore JE (2001). Oral chytridiomycosis in the mountain yellow-legged frog (*Rana muscosa*). *Copeia* **2001**, 945–953.

doi:https://doi.org/10.1643/0045-8511(2001)001%5B0945:OCITMY%5D2.0.CO;2

Fernández-Loras A, Fernández-Beaskoetxea S, Arriero E, Fisher MC, Bosch J (2017). Early exposure to *Batrachochytrium dendrobatidis* causes profound immunosuppression in amphibians. *European Journal of Wildlife Research* **63**. doi:10.1007/s10344-017-1161-y

Garner TWJ, Walker S, Bosch J, Leech S, Marcus Rowcliffe J, Cunningham AA, Fisher MC (2009). Life history tradeoffs influence mortality associated with the amphibian pathogen *Batrachochytrium dendrobatidis*. *Oikos* **118**, 783–791. doi:10.1111/j.1600-0706.2008.17202.x

Gelman A, Jakulin A, Pittau MG, Su Y-S (2008). A weakly informative default prior distribution for logistic and other regression models. *The Annals of Applied Statistics* **2**, 1360–1383. doi:10.1214/08-AOAS191

Gelman A, Meng X-L, Stern H (1996). Posterior predictive assessment of model fitness via realized discrepancies. *Statistica Sinica* **6**, 733–807.

Gog J, Woodroffe R, Swinton J (2002). Disease in endangered metapopulations: the importance of alternative hosts. *Proceedings of the Royal Society B: Biological Sciences* **269**, 671–676. doi:10.1098/rspb.2001.1667

Green PJ (1995). Reversible Jump Markov Chain Monte Carlo computation and Bayesian model determination. *Biometrika* **82**, 711–732. doi:10.2307/2337340

Hagman M, Alford RA (2015). Patterns of *Batrachochytrium dendrobatidis* transmission between tadpoles in a high-elevation rainforest stream in tropical Australia. *Diseases of Aquatic Organisms* **115**, 213–221. doi:10.3354/dao02898

Harjoe CC, Buck JC, Rohr JR, Roberts CE, Olson DH, Blaustein AR (2022). Pathogenic fungus causes density- and trait-mediated trophic cascades in an aquatic community. *Ecosphere* **13**. doi:10.1002/ecs2.4043

Haydon DT, Cleaveland S, Taylor LH, Laurenson MK (2002). Identifying reservoirs of infection: A conceptual and practical challenge. *Emerging Infectious Diseases* **8**, 1468–1473. doi:10.3201/eid0812.010317

Hollanders M (2022). mhollanders/multievent: v1.0. *Zenodo*. doi:https://doi.org/10.5281/zenodo.7024604

Hollanders M, Grogan LF, McCallum HI, Brannelly LA, Newell DA (2023a). Limited impact of chytridiomycosis on juvenile frogs in a recovered species. *Oecologia*. doi:10.1007/s00442-023-05406-w

Hollanders M, Grogan LF, Nock CJ, McCallum HI, Newell DA (2023b). Recovered frog

populations coexist with endemic *Batrachochytrium dendrobatidis* despite load-dependent mortality. *Ecological Applications* **33**, e2724. doi:10.1002/eap.2724

Hyatt AD, Boyle DG, Olsen V, Boyle DB, Berger L, Obendorf D, Dalton A, Kriger K, Hero M, Hines H, Phillott R, Campbell R, Marantelli G, Gleason F, Colling A (2007). Diagnostic assays and sampling protocols for the detection of *Batrachochytrium dendrobatidis*. *Diseases of Aquatic Organisms* **73**, 175–192. doi:10.3354/dao073175

Kéry M, Schaub M (2012). Chapter 7. Estimation of survival from capture-recapture data using the Cormack-Jolly-Seber model. In 'Bayesian Population Analysis Using Winbugs: A Hierarchical Perspective'. pp. 171–239. (Academic Press)

Kilpatrick AM, Briggs CJ, Daszak P (2010). The ecology and impact of chytridiomycosis: an emerging disease of amphibians. *Trends in Ecology & Evolution* **25**, 109–118. doi:10.1016/j.tree.2009.07.011

Knapp RA, Morgan JAT (2006). Tadpole mouthpart depigmentation as an accurate indicator of chytridiomycosis, an emerging disease of amphibians. *Copeia* **2006**, 188–197. doi:10.1643/0045-8511(2006)6[188:TMDAAA]2.0.CO;2

Kriger KM, Hero J-M (2007). Large-scale seasonal variation in the prevalence and severity of chytridiomycosis. *Journal of Zoology* **271**, 352–359. doi:10.1111/j.1469-7998.2006.00220.x

Marantelli G, Berger L, Speare R, Keegan L (2004). Distribution of the amphibian chytrid *Batrachochytrium dendrobatidis* and keratin during tadpole development. *Pacific Conservation Biology* **10**, 173–179. doi:10.1071/PC040173

McElreath R (2020). Chapter 15. Missing data and other opportunities. In 'Statistical rethinking: a Bayesian course with examples in R and Stan'. CRC texts in statistical science. pp. 489–524. (Taylor and Francis, CRC Press: Boca Raton) doi:10.1201/9780429029608

McMahon TA, Rohr JR (2015). Transition of chytrid fungus infection from mouthparts to hind limbs during amphibian metamorphosis. *EcoHealth* **12**, 188–193. doi:10.1007/s10393-014-0989-9

Navarro-Lozano A, Sánchez-Domene D, Rossa-Feres DC, Bosch J, Sawaya RJ (2018). Are oral deformities in tadpoles accurate indicators of anuran chytridiomycosis? *PLOS ONE* **13**, e0190955. doi:10.1371/journal.pone.0190955

Ortiz-Santaliestra ME, Rittenhouse TAG, Cary TL, Karasov WH (2013). Interspecific and postmetamorphic variation in susceptibility of three North American anurans to *Batrachochytrium dendrobatidis*. *Journal of Herpetology* **47**, 286–292. doi:10.1670/11-134

Piotrowski JS, Annis SL, Longcore JE (2004). Physiology of *Batrachochytrium dendrobatidis*, a chytrid pathogen of amphibians. *Mycologia* **96**, 9. doi:10.2307/3761981

R Core Team (2023). R: A language and environment for statistical computing. manual. R Foundation for Statistical Computing, Vienna, Austria. Available at: https://www.R-project.org/

Rachowicz LJ (2002). Mouthpart pigmentation in *Rana muscosa* tadpoles: seasonal changes without chytridiomycosis. *Herpetological Review* **33**, 263–265.

Rachowicz LJ, Briggs CJ (2007). Quantifying the disease transmission function: effects of density on *Batrachochytrium dendrobatidis* transmission in the mountain yellow-legged frog *Rana muscosa*. *Journal of Animal Ecology* **76**, 711–721. doi:10.1111/j.1365-2656.2007.01256.x

Rachowicz LJ, Vredenburg VT (2004). Transmission of *Batrachochytrium dendrobatidis* within and between amphibian life stages. *Diseases of Aquatic Organisms* **61**, 75–83. doi:10.3354/dao061075

Rollins-Smith LA (1998). Metamorphosis and the amphibian immune system. *Immunological Reviews* **166**, 221–230. doi:10.1111/j.1600-065X.1998.tb01265.x

Royle JA, Nichols JD (2003). Estimating abundance from repeated presence-absence data or point counts. *Ecology* **84**, 777–790. doi:10.1890/0012-9658(2003)084[0777:EAFRPA]2.0.CO;2

Sapsford SJ, Alford RA, Schwarzkopf L (2018). Disentangling causes of seasonal infection prevalence patterns: tropical tadpoles and chytridiomycosis as a model system. *Diseases of Aquatic Organisms* **130**, 83–93. doi:10.3354/dao03269

Sauer EL, Cohen JM, Lajeunesse MJ, McMahon TA, Civitello DJ, Knutie SA, Nguyen K, Roznik EA, Sears BF, Bessler S, Delius BK, Halstead N, Ortega N, Venesky MD, Young S, Rohr JR (2020). A meta-analysis reveals temperature, dose, life stage, and taxonomy influence host susceptibility to a fungal parasite. *Ecology* **0**, e02979. doi:10.1002/ecy.2979

Scheele BC, Pasmans F, Skerratt L, Berger L, Martel A, Beukema W, Acevedo AA, Burrowes PA, Carvalho T, Catenazzi A, Foster CN, Frías-Álvarez P, Garner TWJ, Gratwicke B, Guayasamin JM, Hirschfeld M, Kolby JE, Kosch TA, Longo AV, Maneyro R, McDonald CA, Mendelson III JR, Palacios-Rodriguez P, Parra-Olea G, Richards-Zawacki CL, Rödel M-O, Rovito SM, Soto-Azat C, Toledo LF, Voyles J, Weldon C, Whitfield SM, Wilkinson M, Zamudio KR, Canessa S (2019). Amphibian fungal panzootic causes catastrophic and ongoing loss of biodiversity. *Science* **363**, 1459–1463. doi:10.1126/science.aav0379

Stevenson LA, Alford RA, Bell SC, Roznik EA, Berger L, Pike DA (2013). Variation in thermal

performance of a widespread pathogen, the amphibian chytrid fungus *Batrachochytrium dendrobatidis*. *PLoS ONE* **8**, e73830. doi:10.1371/journal.pone.0073830

Stratford D, Grigg G, McCallum H, Hines H (2010). Breeding ecology and phenology of two stream breeding myobatrachid frogs (*Mixophyes fleayi* and *M. fasciolatus*) in south-east Queensland. *Australian Zoologist* **35**, 189–197. doi:10.7882/AZ.2010.007

Symonds EP, Hines HB, Bird PS, Morton JM, Mills PC (2007). Surveillance for *Batrachochytrium dendrobatidis* using *Mixophyes* (Anura: Myobatrachidae) larvae. *Journal of Wildlife Diseases* **43**, 48–60. doi:10.7589/0090-3558-43.1.48

Valencia-Aguilar A, Toledo LF, Vital MVC, Mott T (2016). Seasonality, environmental factors, and host behavior linked to disease risk in stream-dwelling tadpoles. *Herpetologica* **72**, 98–106. doi:10.1655/HERPETOLOGICA-D-15-00013

Venesky MD, Parris MJ, Storfer A (2009). Impacts of *Batrachochytrium dendrobatidis* infection on tadpole foraging performance. *EcoHealth* **6**, 565–575. doi:10.1007/s10393-009-0272-7

Venesky MD, Wilcoxen TE, Rensel MA, Rollins-Smith L, Kerby JL, Parris MJ (2012). Dietary protein restriction impairs growth, immunity, and disease resistance in southern leopard frog tadpoles. *Oecologia* **169**, 23–31. doi:10.1007/s00442-011-2171-1

Voyles J, Johnson LR, Rohr J, Kelly R, Barron C, Miller D, Minster J, Rosenblum EB (2017). Diversity in growth patterns among strains of the lethal fungal pathogen *Batrachochytrium dendrobatidis* across extended thermal optima. *Oecologia* **184**, 363–373. doi:10.1007/s00442-017-3866-8

Wilber MQ, DeMarchi J, Fefferman NH, Silk MJ (2022). High prevalence does not necessarily equal maintenance species: Avoiding biased claims of disease reservoirs when using surveillance data. *Journal of Animal Ecology*, 1365–2656.13774. doi:10.1111/1365-2656.13774

XV Appendix S1: Supplementary figures

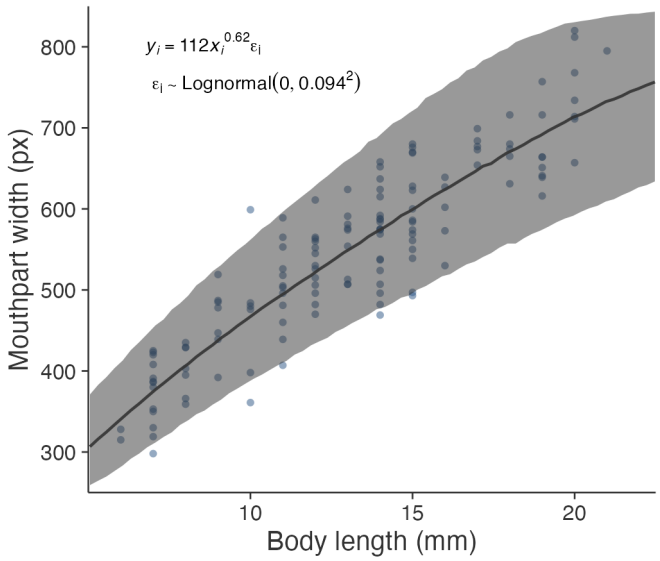

Figure S1: Scatterplot of mouthpart width as measured from photographs in pixels using Adobe Photoshop compared to body length measured with calipers in the field. The posterior predictive distribution (summarised with median and 95% HPDI) is from a log-log regression.

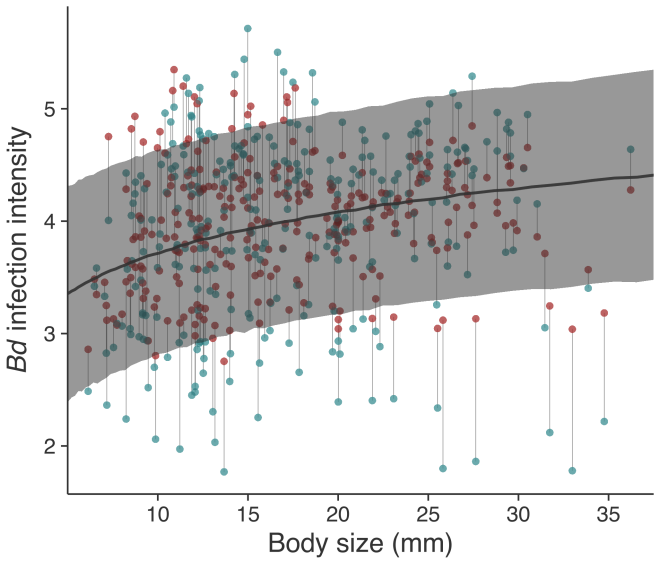

Figure S2: Posterior predictive distribution (summarised with median and 95% HPDI) for the effect of log body size (transformed from mouthpart widths using the equation in Figure S1) on *Bd* infection intensity ($\log_{10}$ gene copies per swab) of *Mixophyes fleayi* tadpoles. Blue points are observed individual *Bd* infection intensities, averaged over positive qPCR runs. Red points are posterior medians of individual infection intensities estimated by the model (m_i, Appendix S2) after propagating measurement error in the sampling (swabbing) and diagnostic (qPCR) processes.

XVI Appendix S2: Statistical analysis of infection prevalence, infection intensity, and mouthpart loss

To identify patterns in *Bd* infection status (infected/uninfected) and infection intensity (pathogen load), we fit a model to swab infection status and ($\log_{10}$) swab loads, respectively, correcting for measurement error in the qPCR and the sampling processes. Our model closely follows the model of DiRenzo *et al.* (2018), except that we used an informative prior for the sampling process measurement error, applied the Royle-Nichols (2003) model for pathogen detection probabilities, and further incorporated mouthpart loss status and intensity as descendant variables from *Bd* infection. Predictors were centered and scaled by two standard deviations to allow direct comparison between binary (site) and continuous (temperature and body size) effects (Gelman *et al.* 2008). We used reversible jump MCMC (RJMCMC, Green 1995) for predictor variable selection and constrained interaction effects to occur in the presence of respective main effects. We ran 4 chains for 50,000 iterations after discarding 10,000 as burn-in and thinning chains by 10, yielding 20,000 posterior samples. We summarised posterior distributions with medians and 95% highest posterior density intervals (HPDI) with RJMCMC inclusion probabilities, and considered effects important when 95% HPDIs of the coefficients did not overlap 0. We conducted posterior predictive checks (PPCs) for all four model components. The fully reproducible analysis is available at https://github.com/mhollanders/mfleayi-tadpoles.

Infection status

We modeled the latent true infection status (z_i) of tadpole $i \in 1, \dots, I = 865$ as a Bernoulli random variable:

$$z_i \sim \text{Bernoulli}\left(\psi_i\right) \tag{1}$$

where the individual probability of being infected with *Bd* (ψ_i) was modeled as a logit-linear function of covariates (site, temperature, log body size, and two/three-way interactions) and random survey effects. Note that 244 missing body size observations were imputed from the distribution of 621 observed values with MCMC.

The observed infection status (y_{ij}, data) during replicate qPCR run $j \in 1, 2$ was modeled—like an occupancy model—as a Bernoulli variable conditional on being infected ($z_i = 1$) and the probability of detecting *Bd* on the infected sample using qPCR (δ_i):

$$y_{ij} \sim \text{Bernoulli}\left(z_i \delta_i\right) \tag{2}$$

where δ_i was modeled as a function of swab infection intensity (n_i, see below), with r being the probability of detecting one $\log_{10}$ *Bd* gene copy on an infected sample in a qPCR run (Royle and Nichols 2003; Hollanders 2022):

$$\delta_i = 1 - (1 - r)^{n_i} \tag{3}$$

Infection intensity

We modeled the latent individual infection intensity (m_i) with a normal linear model:

$$m_i \sim \text{Normal}\left(\mu_i, \sigma_\mu^2\right) \tag{4}$$

where the expected infection intensity (μ_i) was modeled as a linear function of covariates (site, temperature, body size, and covariates) and random survey effects, and σ_μ is the population standard deviation. Random survey effects of infection status and intensity were modeled as draws from a bivariate normal distribution to explore potential correlations.

Knowing that there is measurement error associated with swab samples, but not having replicate samples to estimate this error for tadpoles, we relied on results from replicate samples collected from juveniles (Hollanders 2022) to estimate the sample infection intensity (n_i):

$$n_i \sim \text{Normal}\left(m_i, \sigma_{\text{swab}}^2\right) \tag{5}$$

where the measurement error of the swabbing process (σ_{swab}) was given an informative prior (see Table 1 and **Priors** below).

We modeled the observed infection intensity (x_{ij}, data) during replicate qPCR runs with a normal distribution centered on the sample infection intensity:

$$x_{ij} \sim \text{Normal}\left(n_i, \sigma^2_{\text{qPCR}}\right) \tag{6}$$

where σ_{qPCR} is the measurement error of the qPCR process.

Mouthpart loss

Next, we modeled the observed mouthpart loss status (w_i, data), as determined by the presence of dekeratinisation in either of the two jaw sheaths, as a Bernoulli variable:

$$w_i \sim \text{Bernoulli}\left(\lambda_i\right) \tag{7}$$

where the individual probability of having jaw sheath loss (λ_i) was modeled as a logit-linear function of estimated *Bd* infection status (z_i), *Bd* infection intensity (m_i), separate coefficients for body size with uninfected and infected tadpoles, and random survey effects (survey effects not shown):

$$\text{logit}\,\lambda_i = \alpha_\lambda + \beta_{\lambda_1} z_i + \beta_{\lambda_2} z_i \frac{m_i - \alpha_\mu}{2\sigma_\mu} + \beta_{\lambda_3} z_i \text{size}_i + \beta_{\lambda_4}\left(1 - z_i\right)\text{size}_i \tag{8}$$

Note that the effect of *Bd* infection intensity (β_{λ_2}) was only included for those individuals that were infected ($z_i = 1$), and that infection intensity was centered (by subtracting the average infection intensity α_μ) and scaled by two standard deviations $2\sigma_\mu$. This ensured that the interpretation of β_{λ_1} is the log odds change of having mouthpart loss due to an individual being infected with *Bd* carrying the average infection intensity, and that β_{λ_2} was on the same scale as all other predictors.

Finally, we modeled the observed mouthpart loss intensity (v_i, data), quantified as the sum of the ordinal scores between 1–5 of both the top and bottom jaw sheaths for those individuals where mouthpart loss was detected, as an ordered probit regression with $s \in 1, \ldots, S = 10$ possible scores:

$$
\begin{aligned}
v_i &\sim \text{Categorical}\left(\kappa_{[1\ldots S]_i}\right) \\
\kappa_{[1]_i} &= \Phi\left(\tau_1 - \mu_{\kappa i}\right) \\
\kappa_{[2\ldots S-1]_i} &= \Phi\left(\tau_{[2:S-1]} - \mu_{\kappa i}\right) - \Phi\left(\tau_{[(2\ldots S-1)-1]} - \mu_{\kappa i}\right) \\
\kappa_{[S]_i} &= 1 - \Phi\left(\tau_{[S-1]} - \mu_{\kappa i}\right)
\end{aligned}
\tag{9}
$$

where κ is a probability simplex (summing to 1) of length S, Φ is the cumulative standard normal distribution function (with standard deviation fixed at 1), τ is a vector of $S-1$ thresholds modeled as $\tau_s \sim \text{Normal}\left(\alpha_\tau + \beta_\tau\left(s - S/2\right), \sigma_\tau^2\right)$, and $\mu_{\kappa i}$ is the mean of the standard normal modeled as a linear function of *Bd* infection intensity, body size, and random survey effects (not shown). Infection status was omitted from the model due to the lack of uninfected individuals with mouthpart loss and the resulting poor estimability of that parameter. Random survey effects of mouthpart loss status and intensity were also modeled as correlated using a bivariate normal distribution.

Priors

We used a mixture of vague, weakly informative, and informative priors (Table 1). We specified a $\text{Beta}\left(3,3\right)$ prior for the back-transformed intercept of *Bd* infection status and a weakly informative Student-t prior on the intercept of the log-linear function of infection intensity, centered on the observed average swab infection intensity. We used a conservatively informative $\text{Beta}\left(1,10\right)$ prior on the probability of having mouthpart loss for uninfected tadpoles to reflect the low incidence in the sample (5%). We used weakly informative $t_3\left(0,1\right)$ priors on all coefficients (with predictors standardised by two standard deviations, Gelman *et al.* 2008) to ensure some regularisation and improved MCMC mixing, while allowing for more extreme coefficients. Similarly, we used $t_3^+\left(0,1\right)$ priors on standard deviation parameters, except for the measurement of the swabbing and qPCR processes. Since we did not collect replicate swab samples to estimate this error, we relied on previous work on replicate samples of juvenile *Mixophyes fleayi* from Brindle Creek, using that estimate for a $t_3^+\left(0.17,0.11\right)$ prior (Hollanders 2022). Again, we applied a t prior as the thicker tails allow for deviating values. Although we did have data to estimate the measurement error of the qPCR process, we still used an informative $t_3^+\left(0.5,0.05\right)$ prior because the previous work applied the same diagnostic protocol. We specified a

somewhat informative Beta $(6, 4)$ for the probability of detecting one $\log_{10}$ *Bd* gene copy with qPCR (Hollanders 2022). We applied LKJ (2) priors on the Cholesky factors of the correlation matrices of correlated random survey effects. For the ordinal threshold parameters, we specified a Normal $(0, 1)$ for the intercept τ_α and an Normal$^+$ $(0, 1)$ for τ_β to reflect the constraint that thresholds are ordered. We set a Beta $(1, 1)$ prior for the RJMCMC inclusion probability.

Posterior predictive checks

We conducted PPCs for the *Bd* infection prevalence, infection intensity, and mouthpart loss components of the tadpole model. For each of 20,000 MCMC samples, we simulated replicate infection status (y^{rep}) and intensity (x^{rep}), and mouthpart loss (w^{rep}) and intensity (v^{rep}) datasets from the joint posterior distribution and computed fit statistics for both the observed data and replicate datasets.

For infection status, the binary response was not suitable for test statistics such as χ^2 or Freeman-Tukey statistics, and responses are usually binned across some useful categories as a solution (Kéry and Schaub 2012). In our model, we first summed infection status of individual i across duplicate qPCR run j (y_{ij} and y_{ij}^{rep}) and then binned results for each ($n = 25$) survey $t \in 1, \ldots, T = 25$, yielding y_{survey_t} and $y_{\text{survey}_t}^{\text{rep}}$. For the individual expected value (E_i), we used $2\psi_i\delta_i$ (to incorporate both the latent expected infection prevalence [ψ], the probability of detecting *Bd* [δ], and the number of qPCR runs [2]), which were also summed for each survey, yielding E_{survey_t}. The fit statistics used were Freeman-Tukey statistics calculated for each survey t, leading to the discrepancy measures (D_y and D_y^{rep}) calculated below:

$$\begin{aligned} D_y &= \sum_{t=1}^{25} \left(\sqrt{y_{\text{survey}_t}} - \sqrt{E_{\text{survey}_t}} \right)^2 \\ D_y^{\text{rep}} &= \sum_{t=1}^{25} \left(\sqrt{y_{\text{survey}_t}^{\text{rep}}} - \sqrt{E_{\text{survey}_t}} \right)^2 \end{aligned} \tag{10}$$

For infection intensity, we used χ^2 fit statistics on observed and replicated infection intensity of qPCR runs (x_{ij}) with μ_i as the expectation. The discrepancy measures were the fit statistics summed over all individuals and qPCR runs:

$$
\begin{aligned}
D_x &= \sum_{i=1}^{865} \sum_{j=1}^{2} \frac{\left(x_{ij} - \mu_i\right)^2}{\mu_i} \\
D_x^{\text{rep}} &= \sum_{i=1}^{865} \sum_{j=1}^{2} \frac{\left(x_{ij}^{\text{rep}} - \mu_i\right)^2}{\mu_i}
\end{aligned}
\tag{11}
$$

For mouthpart loss status, we also binned observed and replicated data, along with individual expected value λ_i, across surveys, and calculated Freeman-Tukey statistics, summing across surveys to yield the discrepancy measures:

$$
\begin{aligned}
D_w &= \sum_{t=1}^{25} \left(\sqrt{w_{\text{survey}_t}} - \sqrt{E_{\text{survey}_t}}\right)^2 \\
D_w^{\text{rep}} &= \sum_{t=1}^{25} \left(\sqrt{w_{\text{survey}_t}^{\text{rep}}} - \sqrt{E_{\text{survey}_t}}\right)^2
\end{aligned}
\tag{12}
$$

For mouthpart loss intensity, we used χ^2 statistics on observed and replicated intensity (v_i) with $\sum_{s=1}^{S} \kappa_{s_i} s$ as the expectation, which were subsequently summed over all individuals to arrive at the discrepancy measures:

$$
\begin{aligned}
D_v &= \sum_{i=1}^{865} \sum_{s=1}^{10} \frac{\left(v_i - \sum_{s=1}^{10} \kappa_{s_i} s\right)^2}{\sum_{s=1}^{10} \kappa_{s_i} s} \\
D_v^{\text{rep}} &= \sum_{i=1}^{865} \sum_{s=1}^{10} \frac{\left(v_i^{\text{rep}} - \sum_{s=1}^{10} \kappa_{s_i} s\right)^2}{\sum_{s=1}^{10} \kappa_{s_i} s}
\end{aligned}
\tag{13}
$$

We then visually inspected the discrepancies by plotting the discrepancy of the simulated datasets against the discrepancy of the observed dataset for all 20,000 MCMC samples (Figure S3), and calculated the Bayesian p-values (BPVs) as the proportion of samples where the discrepancy of simulated data was greater than the discrepancy of the observed data ($\Pr\left(D^{\text{rep}} > D\right)$).

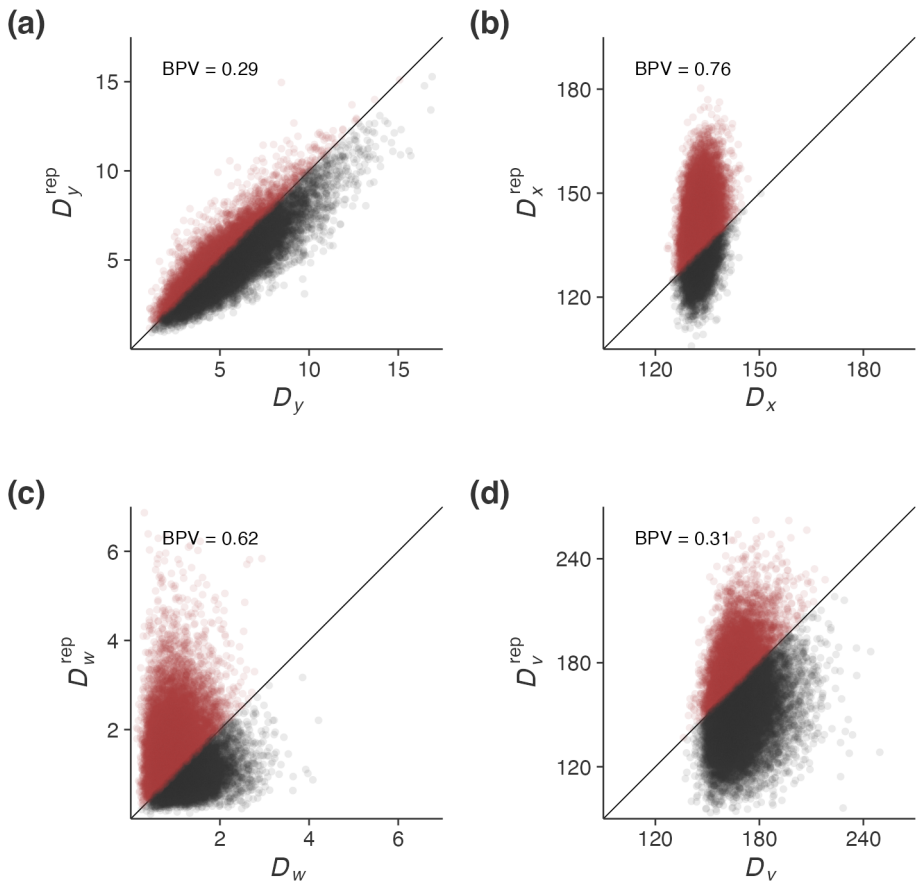

Figure S3: Discrepancy measures from simulated datasets (D^{rep}) versus observed data (D) for each of 20,000 MCMC samples for **(a)** *Bd* infection prevalence (calculated from Freeman-Tukey statistics), **(b)** *Bd* infection intensity (calculated from χ^2 statistics), **(c)** mouthpart loss status (calculated from Freeman-Tukey statistics), and **(d)** mouthpart loss intensity (calculated from χ^2 statistics). Bayesian p-values (BPVs) are the proportion of MCMC samples for which the discrepancy of replicated data was greater than the discrepancy of the observed data ($\Pr(D^{\text{rep}} > D)$). The color red indicates when $D^{\text{rep}} > D$.